The effect of parameterization on isogeometric analysis of free-form curved beams

Seyed Farhad Hosseini, Behnam Moetakef-Imani, Saeid Hadidi-Moud & Behrooz Hassani

Acta Mechanica

ISSN 0001-5970
Volume 227
Number 7

Acta Mech (2016) 227:1983-1998
DOI 10.1007/s00707-016-1610-9

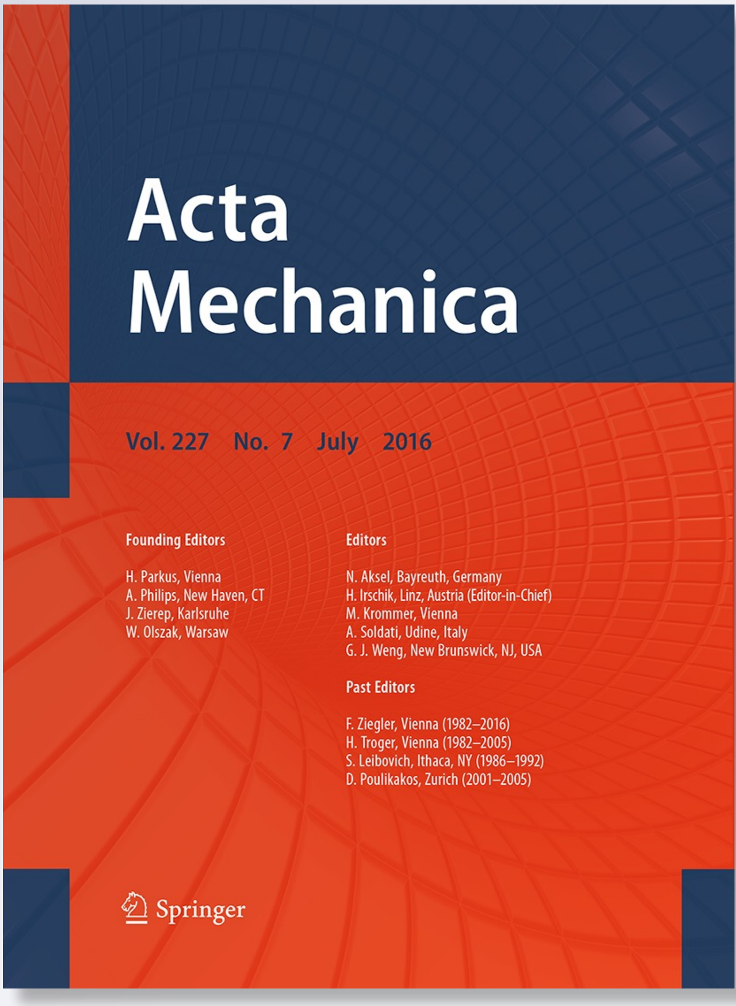

Springer

Acta Mech 227, 1983–1998 (2016)
DOI 10.1007/s00707-016-1610-9

ORIGINAL PAPER

Seyed Farhad Hosseini · Behnam Moetakef-Imani ·
Saeid Hadidi-Moud · Behrooz Hassani

The effect of parameterization on isogeometric analysis of free-form curved beams

Received: 10 October 2015 / Revised: 25 February 2016 / Published online: 6 April 2016

Abstract In the present paper, the effect of parameterization on the results of isogeometric analysis of free-form approximated curved beams is investigated. An Euler–Bernoulli beam element for an initially curved beam with variable curvature is developed. The model is applied to four different examples. The effect of three parameterization strategies (the equally spaced method, the chord length method and the centripetal method) in the curve approximation process is considered. Also, the effect of least square approximation error is taken into consideration. The results strongly suggest avoiding the equally spaced method. Among the chord length and centripetal methods, the method which leads to a less least square error is recommended.

1 Introduction

The concept of isogeometric analysis (IGA) was first introduced by Hughes et al. [1]. It can be viewed and interpreted as a logical extension to the finite element method. The method employs shape functions based on different types of splines (B-spline, NURBS, T-splines, etc.). The main feature of this approach is that the shape functions not only represent the CAD geometry, but also are considered as a basis for the numerical approximation of the solution space. IGA integrates finite element ideas in commercial CAD systems without the necessity to generate new computational meshes. This approach was successfully applied to a wide range of physical problems such as solid mechanics [2–4], fluid mechanics [5], heat transfer [6] and eigenvalue problems [7].

Very recently, the isogeometric analysis of curved beams has attracted many researchers. Bouclier et al. [8] investigated the use of higher-order NURBs to address static straight and curved Timoshenko beams with several approaches that are usually employed in standard locking-free finite elements. Nagy et al. [9] studied sizing and shape optimization of curved beams using IGA. Cazzani et al. [10] presented a plane curved beam element which is almost insensitive to both membrane and shear locking. They stated that membrane and shear locking phenomena can be easily controlled by either properly choosing the number of elements or the NURBs degree.

In general, a free-form curve can be constructed from arbitrary input data points using interpolation or approximation methods [11]. In interpolation, the curve is precisely passed through all data points, while in approximation, the least square error between data points and their corresponding points on the curve is minimized.

S. F. Hosseini · B. Moetakef-Imani · S. Hadidi-Moud · B. Hassani
Department of Mechanical Engineering, Ferdowsi University of Mashhad (FUM), Mashhad, Iran

B. Moetakef-Imani (✉)
Ferdowsi University of Mashhad (FUM) Campus, Azadi Sq., P.O. Box: 9177948974,
Mashhad, Khorasan Razavi, Iran
E-mail: imani@um.ac.ir
Tel.: +989151133175

In the work done by Luu et al. [12], the gap between the free vibration isogeometric analysis of curved beams with constant curvature and those with variable curvature is eliminated. They considered a Tschirnhausen cubic curved beam configuration to study the dynamic behavior of a free-form curved beam. There exist different types of interpolation and approximation methods distinguished by their different parameterization methods. Two visually identical curves may have different parameterizations which lead to different control points and knot vectors. One can interpret the parameterization as a "hidden" concept that can affect the results of IGA. Different parameterizations will lead to different discretizations which can in turn cause mesh distortion. Mesh distortion is a serious problem in both FEA and IGA. Kolman [13] tested two types of parameterizations for a straight line: a nonlinear parameterization given by uniformly spaced control points and a linear parameterization as a result of employing the Greville abscissa.

Cotrell et al. [14] showed that the nonlinear parameterization is superior for outlier frequencies. Other researchers [15] have investigated the effect of perturbing control points in one-dimensional setting and extended this concept to multiple dimensions. Perturbing a control point in one-dimensional setting would change the parameterization, whereas the line is visually unchanged. Although there exists a series of studies briefly addressing the effect of parameterization [16–19], a much needed comprehensive research focusing on the effect of parameterization on free-form approximated (interpolated) curved beam is necessary. Therefore, the present work aims to provide a sound insight into this concept based on IGA.

The article is organized as follows: Firstly, in Sect.2 a brief introduction into B-spline and NURBs functions is presented and the interpolation and approximation methods as well as three parameterization techniques are introduced. After that, the formulation of isogeometric analysis of free-form (variable curvature) curved beams is presented in Sect. 3. This formulation is adopted from the concept of shell isogeometric element developed in [20]. In Sect. 4, the effect of parameterization on isogeometric analysis of curved beams is shown and a complete discussion on the results is given. The effect of zero continuity in the geometry is also addressed in Sect. 5. Finally Sect. 6 concluded the discussions.

2 Basic definitions

B-spline curve and surface algorithms required for implementing into isogeometric analysis are briefly introduced in this section.

2.1 B-spline curves and surfaces

B-spline theory is a parametric method of describing curves and surfaces. Outstanding properties and programming capabilities have made the method popular for CAD/CAM applications. A clamped B-spline curve is a piecewise polynomial which is expressed by

$$C\left(u\right)=\sum_{i=0}^{n}N_{i,p}\left(u\right)P_i, \tag{1}$$

where p is the degree and $P_i, i=0,..,n$ is the control polygon which is defined by $P_i=(x_i,y_i,z_i)$.The term $N_{i,p}\left(u\right), i=0,\ldots,n$ represents B-spline basis functions that are defined on the knot vector, U:

$$U=\left\{\underbrace{0,\ldots,0}_{p+1},u_{p+1},\ldots,u_{m-p-1},\underbrace{1,\ldots,1}_{p+1}\right\}. \tag{2}$$

The extension of B-spline theory to a tensor product of two B-spline curves results in a definition for B-spline surface, S:

$$S\left(u,v\right)=\sum_{i=0}^{n}\sum_{j=0}^{m}N_{i,p}\left(u\right)N_{j,q}\left(v\right)P_{i.j} \tag{3}$$

where p and q are surface degrees in the u and v directions, respectively, and $P_{i,j}\ (i=0,\ldots,n;\ j=0,\ldots,m)$ is a net of control points defined as $P_{i,j}=\left(x_{i,j},y_{i,j},z_{i,j}\right)$. Also $N_{i,p}\left(u\right),\ i=0,\ldots,n$ and $N_{j,q}\left(v\right),\ j=$

$0, \ldots, m$ are B-spline basis functions in the u and v directions which are defined on the following knot vectors, respectively:

$$U = \left\{ \underbrace{0, \ldots, 0}_{p+1}, u_{p+1}, \ldots, u_{r-p-1}, \underbrace{1, \ldots, 1}_{p+1} \right\},$$
$$V = \left\{ \underbrace{0, \ldots, 0}_{q+1}, v_{q+1}, \ldots, v_{s-q-1}, \underbrace{1, \ldots, 1}_{q+1} \right\}. \tag{4}$$

Further details of B-spline curves and surfaces can be found in [11].

2.2 Approximation of curves and surfaces

Three necessary stages should be passed on to obtain an approximated surface

(a) Selecting proper parameter for each data point
(b) Generating a proper knot vector
(c) Calculating control points as the output of problem

There are several methods to fulfill each of the above stages. What are going on are formulations related to a specific method which has been used in this work.

2.2.1 Parameter selection

Parameters are in fact the reflection of distribution of data points. Three parameterization techniques, the equally spaced, chord length and centripetal methods, are used for most applications. The input data points and their corresponding parameters are denoted by Q_i, $i = 0, \ldots, k$, and t_i, $i = 0, \ldots, k$. Thus, the evaluated point on the approximated curve at t_i is equal to Qi.

In the equally spaced method:

$$\begin{cases} t_0 = 0 \\ t_i = i/k \\ t_k = 1 \end{cases} \tag{5}$$

In the chord length method data point parameters are calculated by:

$$\begin{cases} t_0 = 0 \\ t_i = t_{i-1} + \frac{|Q_i - Q_{i-1}|}{L} \\ t_k = 1 \end{cases} \tag{6}$$

where

$$L = \sum_{i=1}^{k} |Q_i - Q_{i-1}|.$$

And for the centripetal method, parameters may be obtained by:

$$\begin{cases} t_0 = 0 \\ t_i = t_{i-1} + \frac{\sqrt{|Q_i - Q_{i-1}|}}{L} \\ t_k = 1 \end{cases} \tag{7}$$

where

$$L = \sum_{i=1}^{k} \sqrt{|Q_i - Q_{i-1}|}.$$

2.2.2 knot vector generation

Several methods are suggested for knot vector selection, among them, the following algorithm is usually preferred and implemented [11]:

$$\begin{aligned} d &= \frac{k+1}{n-p+1} \\ i &= \operatorname{int}(jd), \quad \alpha = jd - i \\ u_{p+j} &= (1-\alpha)\,\bar{u}_{i-1} + \alpha\bar{u}_i, \quad j = 1, \ldots, n-p \end{aligned} \tag{8}$$

where k is the number of data points, n is the number of control points, and p is the degree of the B-spline. The "int" command gives the largest integer smaller than its input real number. The above algorithm will ensure that there are a specific and almost equal number of parameters between each two consecutive middle knots which plays an important role in the stability of solutions [21].

2.2.3 Least square approximation

In the least square method, the following error function is to be minimized:

$$\sum_{i=1}^{k-1} |Q_i - C(t_i)|^2 \tag{9}$$

which leads to the following system of equations [11]:

$$\left(N^T N\right) P = R, \tag{10}$$

where N is a $(n-1)$ by $(k-1)$ matrix:

$$\begin{bmatrix} N_{1,p}(t_1) & \cdots & N_{n-1,p}(t_1) \\ \vdots & \ddots & \vdots \\ N_{1,p}(t_{k-1}) & \cdots & N_{n-1,p}(t_{k-1}) \end{bmatrix} \tag{11}$$

and R is a $(n-1)$ vector:

$$\begin{bmatrix} N_{1,p}(t_1)\,R_1 + \ldots + N_{1,p}(t_{k-1})\,R_{k-1} \\ \vdots \\ N_{n-1,p}(t_1)\,R_1 + \ldots + N_{n-1,p}(t_{k-1})\,R_{k-1} \end{bmatrix} \tag{12}$$

R_i is defined by:

$$R_i = Q_i - N_{0,p}(t_i)\,Q_0 - N_{n,p}(t_i)\,Q_k \quad , i = 1, \ldots, k-1. \tag{13}$$

It should be noted that P, the vector of control points, is the unknown of the problem.

3 Isogeometric analysis of plane free-form curved beams

For the description of free-form curves, it is advantageous to use curvilinear coordinates and local bases as depicted in Fig. 1, where the vectors $\vec{\boldsymbol{A}}$ and $\vec{\boldsymbol{a}}$ are the base vectors in the reference and current configurations, respectively. The deformation of a thin, elastic and uniform Euler–Bernoulli beam is comprised of membrane and flexural components. The position of each point on the deformed beam (Fig. 2) can be expressed using the following relations:

$$x\left(\theta^1, \theta^2\right) = r\left(\theta^1\right) + \theta^2 a_2\left(\theta^1\right), \tag{14}$$

where θ^1 and θ^2 are curvilinear coordinates and r is the position vector of corresponding point on the midline of the beam. The director $\overrightarrow{\boldsymbol{a}_2}$ can be written as

$$a_2 = A_2 + \Phi \times A_2, \tag{15}$$

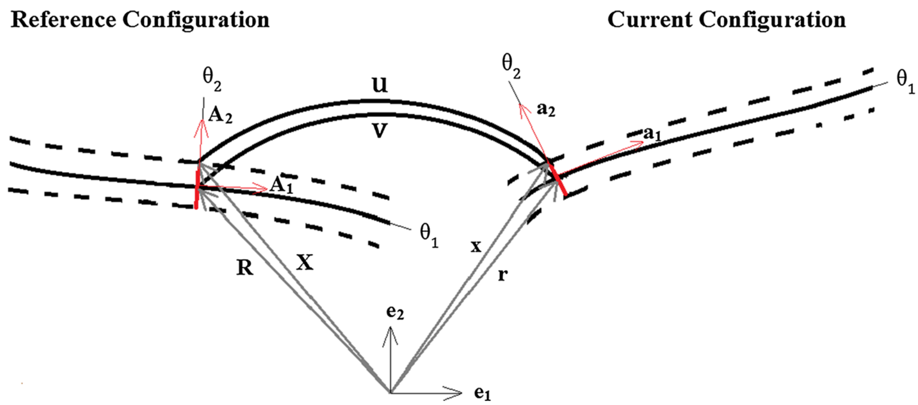

Fig. 1 Curved beam configurations in reference and deformed (current) states

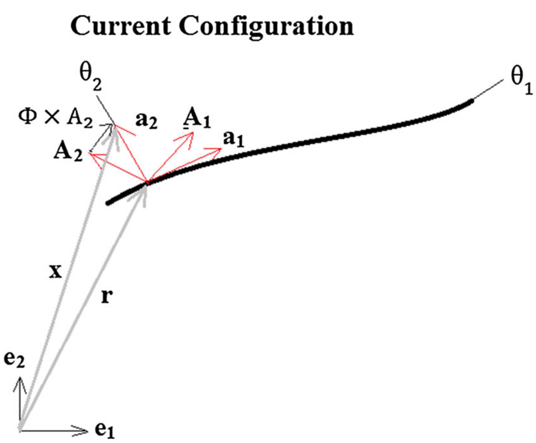

Fig. 2 A curvilinear configuration

where Φ is the rotation vector. Considering the rotation angle, the rotation vector can be written as

$$\Phi = \varphi A_3. \tag{16}$$

In this equation, A_3 is the normal to plane vector and φ is the rotation angle and can be obtained using the following equation:

$$\varphi = v_{,1}.A_2, \tag{17}$$

where $v_{,1}$ is the partial derivative of midline displacement field, v, of the beam with respect to the coordinate θ^1. The difference between position vectors x and X will lead to a displacement field u at each point of a plane curved beam:

$$u = x - X. \tag{18}$$

The derivation of the Green–Lagrange strain tensor coefficients ε_{ij} requires partial derivatives of the displacement field u with respect to the coordinate θ^1:

$$u_{,1} = v_{,1} + \theta^2 \left(\Phi_{,1} \times A_2 + \Phi \times \mathrm{A}_{2,1}\right). \tag{19}$$

Considering the finite Green–Lagrange formula, the individual strain can be obtained as follows:

$$\varepsilon_{11} = v_{,1} A_1 + \theta^2 \left(v_{,1}.A_{2,1} + \Phi_{,1} \times A_2.A_1\right). \tag{20}$$

With the strain component of Eq. (20), the internal virtual work of the Euler–Bernoulli beam can be defined:

Fig. 3 The configuration of a cantilever straight beam

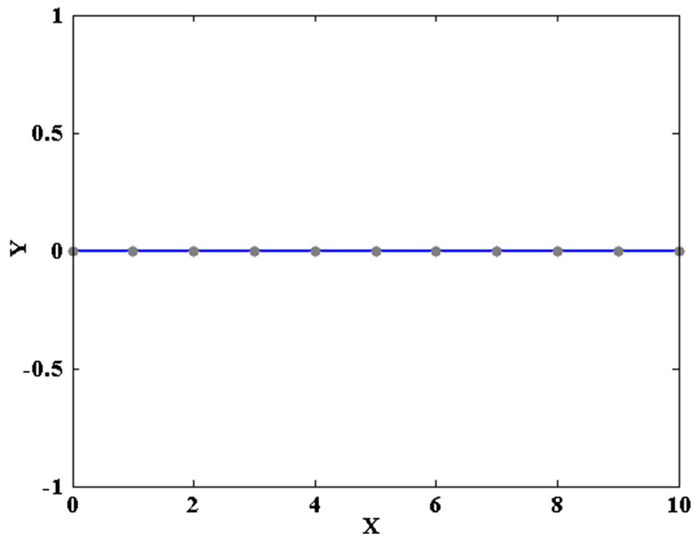

Fig. 4 The input data points of a cantilever straight beam

$$\delta\pi = \int_{\Omega} \delta(\varepsilon)^T C\varepsilon d\Omega, \tag{21}$$

where C is the material property coefficient.

In IGA, this discretization is performed using the B-spline and NURBs functions. According to the isoparametric concept, the discrete displacement field of the midline, v, is determined from the sum of NURBs element basis functions and associated displacements of the control points as follows:

$$v(\xi) = \sum_{i=1}^{n_{cp}} N_i^p(\xi)\ v^i, \tag{22}$$

where n_{cp} is the number of control points, ξ is the parameter, p is the B-spline degree, N_i^p are the basis functions, and finally, v^i are control point values.

As much as the vector A_1 is always tangent to the curve, it can be written as

$$A_1(\xi) = \sum_{i=1}^{n_{cp}} N_i^P(\xi)_{,\xi}\ P^i, \tag{23}$$

where P^i are the control points of the input geometry. The problem unknowns $\left(v^i\right)$ are computed by discretization of Eq. (21) using Eqs. (20), (22) and (23).

4 Results and discussion

The effect of parameterization on the isogeometric analysis of free-form curved beams was investigated. A free-form curve can be constructed from a set of data points using approximation and interpolation techniques. As described in Sect. 2, there are various parameterization methods which may lead to visually identical, yet intrinsically different curves, because they have different control points and different knot vectors.

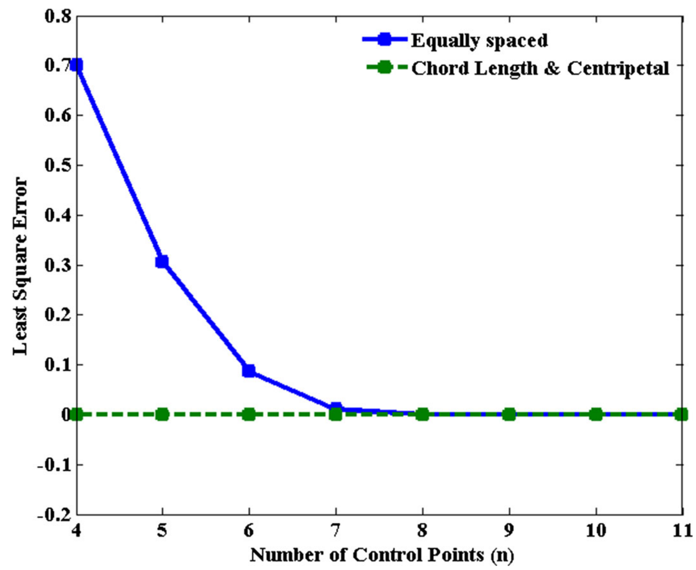

Fig. 5 Least square error versus the number of control points for different types of parameterization in Example 1

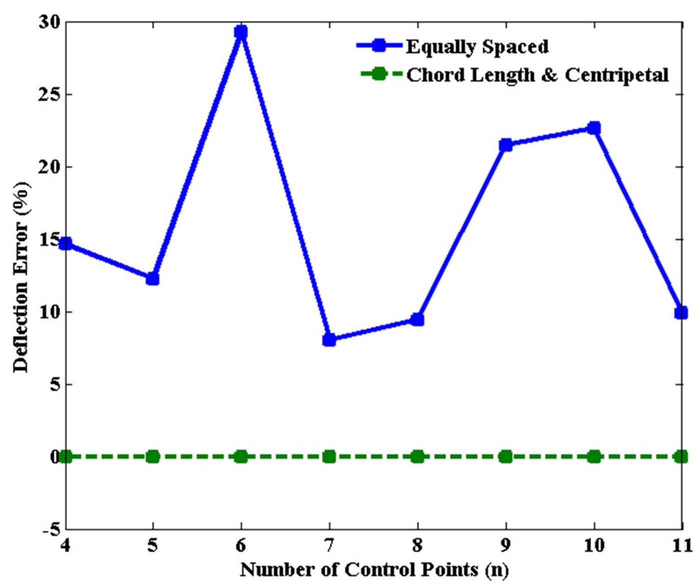

Fig. 6 Tip deflection error versus the number of control points for different types of parameterization in Example 1

The curved beam isogeometric analysis was performed on four benchmark examples. In all examples, the number of meshes can be altered by employing different number of control points as an approximation (interpolation) input. For comparison purposes, the variation of the approximation least square error is also plotted versus the number of control points. The results are reported in the subsequent sections.

Example 1 A cantilever straight beam.

The configuration and input data points are shown in Figs. 3 and 4, respectively. Since the input data points are uniformly distributed, the error outputs for chord length and centripetal approximations are the same.

The variation of least square and tip deflection errors versus the number of control points is depicted in Figs. 5 and 6, respectively.

Example 2 A quarter circular in-plane cantilever curved beam.

Figures 7 and 8 show the configuration and input data points of a cantilever quarter circle beam. The data points are again uniformly distributed; hence, the chord length and centripetal outputs are identical.

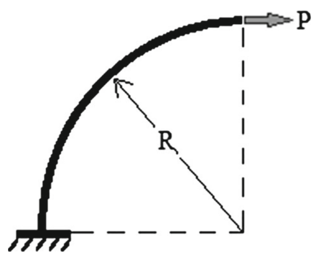

Fig. 7 The configuration of a quarter circular in-plane cantilever curved beam

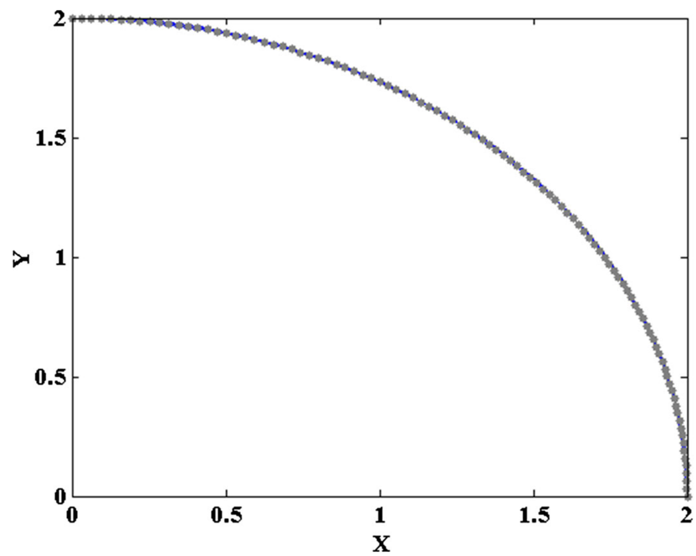

Fig. 8 The input data points of the beam in Example 2

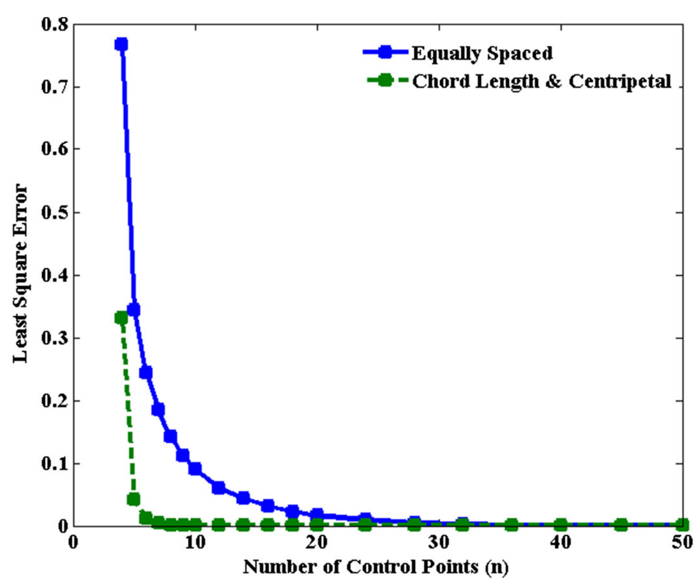

Fig. 9 Least square error versus the number of control points for different types of parameterization in Example 2

The variation of least square and vertical tip deflection errors versus the number of control points is depicted in Figs. 9 and 10, respectively.

Example 3 A cantilever quarter circular in-plane curved beam with non-uniform input data points.

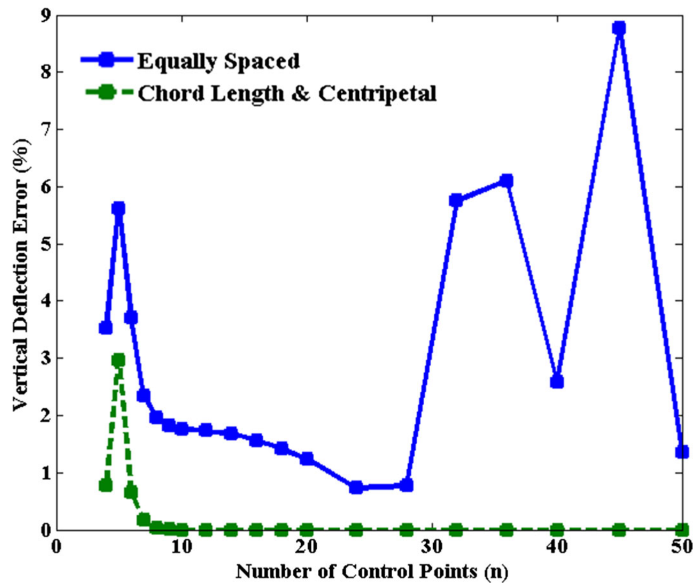

Fig. 10 Vertical tip deflection error versus the number of control points for different types of parameterization in Example 2

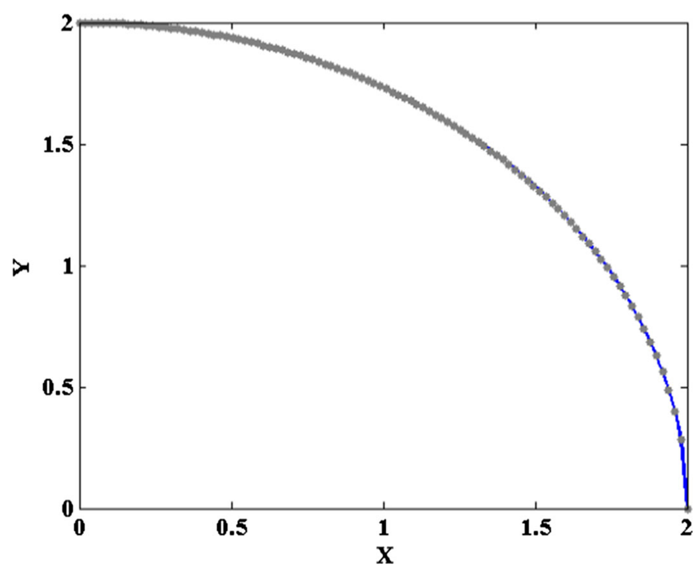

Fig. 11 The non-uniform input data points of the beam in Example 3

This example is devised to investigate the effect of non-uniform input data points. The configuration is similar to the previous example, with the exception of the distribution of data points which is different as shown in Fig. 11.

The variation of least square and vertical tip deflection errors versus the number of control points is depicted in Figs. 12 and 13, respectively.

Example 4 A cantilever Tschirnhausen plane curved beam.

To take the curvature variation into consideration, the Tschirnhausen curve was considered. The configuration is demonstrated in Fig. 14.

The data points were calculated from the following Tschirnhausen parametric equation:

$$x = 3a\left(t^2 - 3\right),$$
$$y = ta\left(t^2 - 3\right).$$

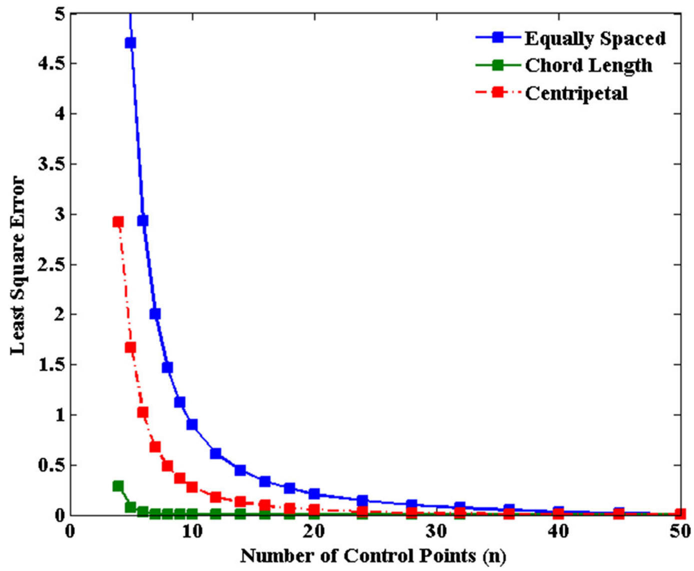

Fig. 12 Least square error versus the number of control points for different types of parameterization in Example 3

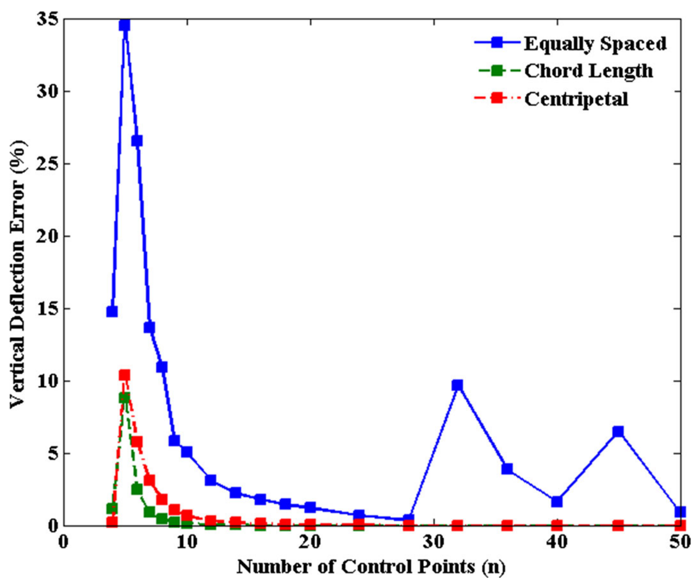

Fig. 13 Vertical tip deflection error versus the number of control points for different types of parameterization in Example 3

Fig. 14 The configuration of a Tschirnhausen cantilever beam used in Example 4

Choosing $a = 1$, the data points are shown in Fig. 15.

Considering this geometry as a cantilever beam, with a clamped edge at right, the variation of least square and tip deflection errors versus the number of control points is demonstrated in Figs. 16 and 17.

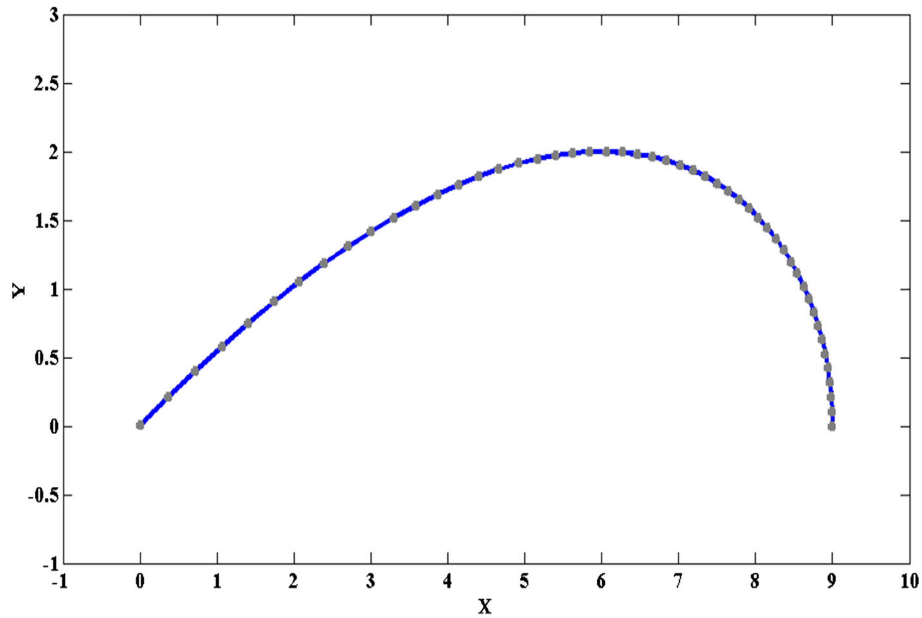

Fig. 15 The input data points of a Tschirnhausen curve

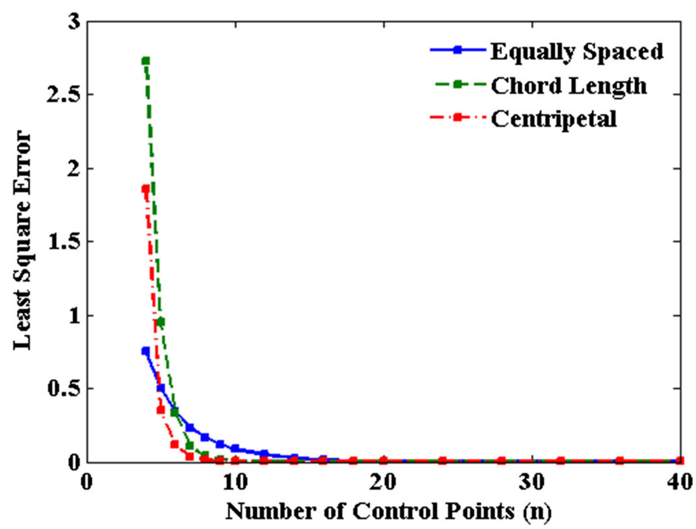

Fig. 16 Least square error versus the number of control points for different types of parameterization in Example 4

4.1 Effect of arc-length parameterization

Parameterization has a significant influence on the mesh distortion of the geometry. With a linear parameterization, the arc-length mapping from a model space into its parameter space is achieved. In this case, the Jacobian corresponding to this mapping is constant [15]. These characteristics of the arc-length parameterization were evaluated for all examples considered in this work. For a fixed number of control points, the variation of model coordinate, X, and Jacobian versus the B-spline parameter for different parameterization approaches is shown in Figs. 18 and 19 for Example 1.

From these figures, it is clear that the chord length and centripetal parameterizations are more likely to lead to a linear (or arc-length) parameterization.

However, centripetal parameterization is not always linear. Figure 20 shows the plot of the Jacobian versus the spline parameter for Example 4.

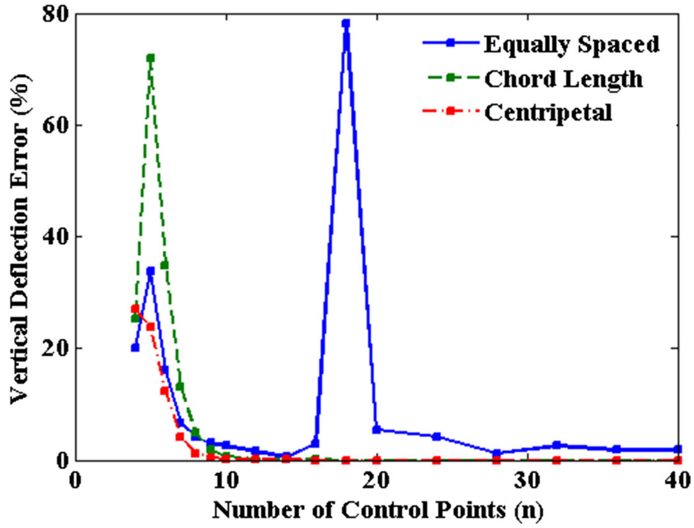

Fig. 17 Vertical tip deflection error versus the number of control points for different types of parameterization in Example 4

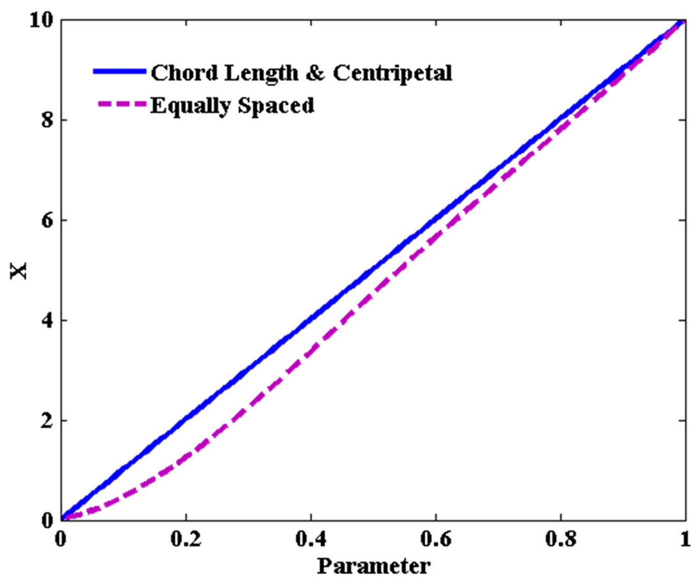

Fig. 18 Plot of the parameterization for the cases of equally spaced and Chord length parameterizations for Example 1

Although the centripetal parameterization is not linear in this example, its deflection error is slightly smaller than the chord length parameterization (Fig. 17). This may be due to the fact that centripetal parameterization, like chord length parameterization, takes the initial distribution of data points into consideration.

Considering this fact, we can conclude that in most cases, mesh distortion in chord length and centripetal parameterizations is generally less than equally spaced parameterization; hence, chord length and centripetal parameterizations give more accurate results.

4.2 Effect of the least square approximation error

In general, less error of the least square approximation leads to less deflection errors. However, this is not always true as it depends on the parameterization method used. By careful observation of Figs. 12 and 13, one can find out that an equally spaced parameterization with 32 control points has led to less approximation error than a centripetal parameterization with 5 control points, whereas the deflection error of the latter is less.

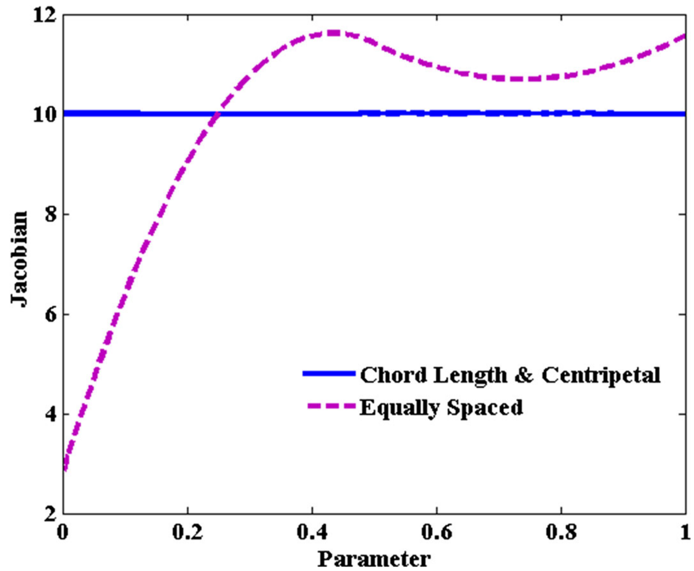

Fig. 19 Plot of the Jacobian of the parameterization for the cases of uniformly spaced control points and linear parameterization for Example 1

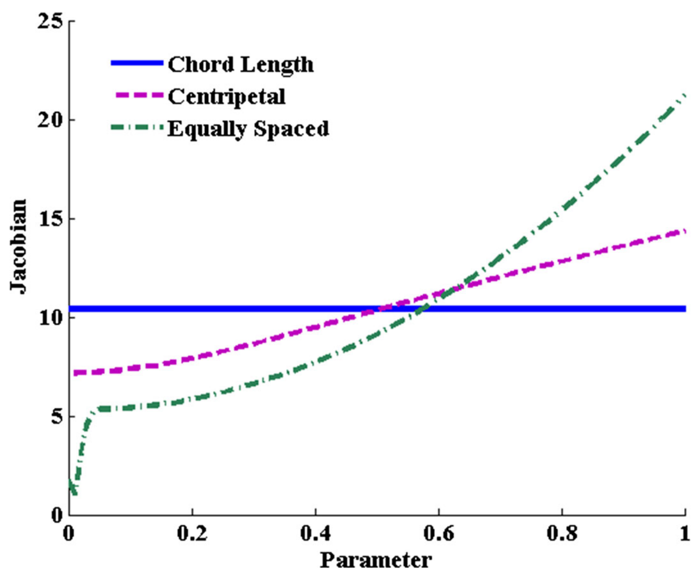

Fig. 20 Plot of the Jacobian of the parameterization for all parameterization methods for Example 4

Moreover, there is not a uniform relation between the least square error and the deflection error for the equally spaced procedure.

By careful examination of the results obtained for Example 4, it is suggested that the convergence rate of centripetal method in variable curvature problems is faster than the chord length method. This may be due to the fact that the convergence of the approximation least square error to zero in centripetal method is faster than in the chord length method. On the other hand, in Example 3, where non-uniform input points were introduced, the chord length method is superior. This is because at a fixed number of control points its least square error is less than the error in centripetal method. Therefore, it may be concluded that between the chord length and centripetal methods, the one which leads to less approximation error is more likely to also lead to less deflection error.

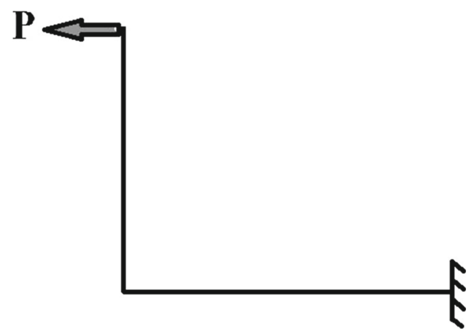

Fig. 21 The configuration of L-shape beam Example

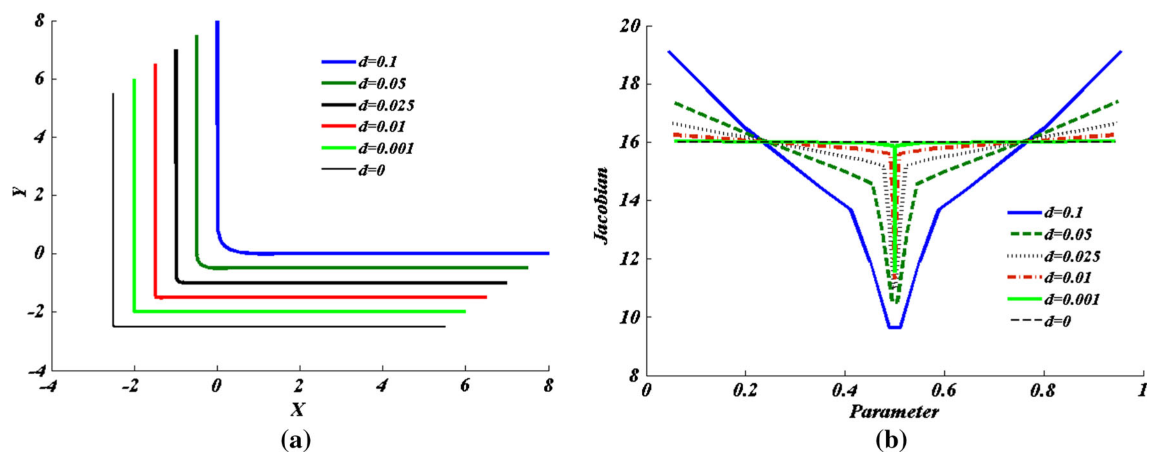

Fig. 22 The effect of decreasing d on **a** geometry and **b** Jacobian

5 Effect of C^0 continuity

In this section, a numerical test is designed to assess the effect of zero continuity on the results of IGA. The configuration of this test is shown in Fig. 21.

Control points and the knot vector of the cubic B-spline are assigned as follows:

$$\begin{aligned}&\text{Control points: }\{(8,0)\ (16/3,0)\ (8/3,0)\ (0,0)\ (0,8/3)\ (0,16/3)\ (0,8)\}\\&\text{Knot vector: }\ \{0,0,0,0,0.5-d,0.5,0.5+d,1,1,1,1\}\end{aligned} \tag{24}$$

where d is a parameter considered for analyzing the effect of C^0 continuity on the IGA results. Decreasing d from 0.1 to 0 results in variations of geometry and Jacobian as illustrated in Fig. 22. It should be noted that to better understand the effect of decreasing d on the corner, each curve is translated by a constant vector in Fig. 22a.

It is demonstrated in Fig. 22b that at exact value of d equal to 0, an arc-length L-shape curve with C^0 continuity is obtained.

At $u = 0.5$, the tangent vector (A_1) is undefined; hence, the curve is singular at this point. Such problems may be solved in the vicinity of the C^0 junction point. As d approaches 0, the deflection errors (compared to the analytical results) approach 0, see Fig. 23.

It can be concluded that for a beam with a breaking point, in addition to the essential parameterization considerations, it is required to define the knot vector as expressed in Eq. (24) and solve for desired values as d approaches 0.

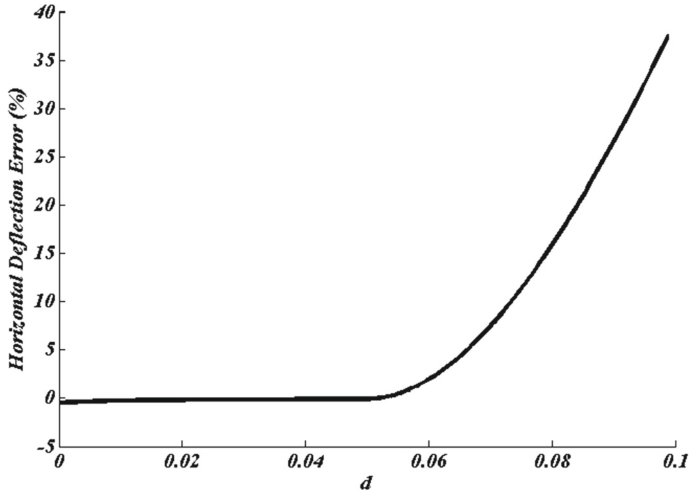

Fig. 23 Variation of the horizontal deflection error versus d

6 Conclusions

- The effect of parameterization and least square approximation error on isogeometric analysis results of free-form curved beams was considered.
- Implementing "chord length" and "centripetal" parameterizations showed that by increasing the accuracy of approximation, i.e., increasing the number of approximation control points, the accuracy of isogeometric results was also increased.
- Implementing "equally spaced" approximation suggested that increasing the accuracy of approximation did not necessarily lead to more accurate results.
- "Chord length" and "centripetal" approaches that reflect the initial distribution of input points resulted in more accurate results. Therefore, it could not be concluded that use of a linear parameterization would always result in more accurate IGA solutions.
- The authors highly suggest avoiding equally spaced parameterization for IGA. Among the chord length and centripetal methods, the authors recommend the method which results in a less least square error.
- For a beam with a breaking point, in addition to the essential parameterization considerations, it is required to solve the problem in the vicinity of the C^0 junction point.

References

1. Hughes, T.J.R., Cottrell, J.A., Bazilevs, Y.: Isogeometric analysis: CAD, finite elements, NURBS, exact geometry and mesh refinement. Comput. Methods Appl. Mech. Eng. **194**(39–41), 4135–4195 (2005)
2. Hassani, B., Taheri, A.H., Moghaddam, N.Z.: An improved isogeometrical analysis approach to functionally graded plane elasticity problems. Appl. Math. Modell. **37**(22), 9242–9268 (2013)
3. Nagy, A.P., Ijsselmuiden, S.T., Abdalla, M.M.: Isogeometric design of anisotropic shells: optimal form and material distribution. Comput. Methods Appl. Mech. Eng. **264**, 145–162 (2013)
4. Moosavi, M.-R., Khelil, A.: Isogeometric meshless finite volume method in nonlinear elasticity. Acta Mech. **226**, 123–135 (2014)
5. Motlagh, Y.G., Ahn, H.T., Hughes, T.J.R., Calo, V.M.: Simulation of laminar and turbulent concentric pipe flows with the isogeometric variational multiscale method. Comput. Fluids **71**, 146–155 (2013)
6. Yoon, M., Ha, S.-H., Cho, S.: Isogeometric shape design optimization of heat conduction problems. Int. J. Heat Mass Transf. **62**, 272–285 (2013)
7. Shojaee, S., Izadpanah, E., Valizadeh, N., Kiendl, J.: Free vibration analysis of thin plates by using a NURBS-based isogeometric approach. Finite Elem. Anal. Des. **61**, 23–34 (2012)
8. Bouclier, R., Elguedj, T., Combescure, A.: Locking free isogeometric formulations of curved thick beams. Comput. Methods Appl. Mech. Eng. **245–246**, 144–162 (2012)
9. Nagy, A.P., Abdalla, M.M., Gürdal, Z.: Isogeometric sizing and shape optimisation of beam structures. Comput. Methods Appl. Mech. Eng. **199**(17–20), 1216–1230 (2010)
10. Cazzani, A., Malagu, M., Turco, E.: Isogeometric analysis of plane-curved beams. math. mech. solids **1**, 1–16 (2014)
11. Piegl, L., Tiller, W.: The NURBS Book, 2nd edn. Springer, Berlin (1996)

12. Luu, A.-T., Kim, N.-I., Lee, J.: Isogeometric vibration analysis of free-form Timoshenko curved beams. Meccanica **50**(1), 169–187 (2015). doi:10.1007/s11012-014-0062-3
13. Kolman, R.: Isogeometric free vibration of an elastic block. Eng. MECHANICS **19**(4), 279–291 (2012)
14. Cottrell, J.A., Reali, A., Bazilevs, Y., Hughes, T.J.R.: Isogeometric analysis of structural vibrations. Comput. Methods Appl. Mech. Eng. **195**(41–43), 5257–5296 (2006)
15. Lipton, S., Evans, J.A., Bazilevs, Y., Elguedj, T., Hughes, T.J.R.: Robustness of isogeometric structural discretizations under severe mesh distortion. Comput. Methods Appl. Mech. Eng. **199**(5–8), 357–373 (2010)
16. Shojaee, S., Valizadeh, N., Izadpanah, E., Bui, T., Vu, T.-V.: Free vibration and buckling analysis of laminated composite plates using the NURBS-based isogeometric finite element method. Compos. Struct. **94**(5), 1677–1693 (2012)
17. Kolman, R., Plešek, J., Okrouhlík, M.: Complex wavenumber Fourier analysis of the B-spline based finite element method. Wave Motion **51**(2), 348–359 (2014)
18. Cohen, E., Martin, T., Kirby, R.M., Lyche, T., Riesenfeld, R.F.: Analysis-aware modeling: understanding quality considerations in modeling for isogeometric analysis. Comput. Methods Appl. Mech. Eng. **199**(5–8), 334–356 (2010)
19. Hughes, T.J.R., Reali, A., Sangalli, G.: Duality and unified analysis of discrete approximations in structural dynamics and wave propagation: Comparison of p-method finite elements with k-method NURBS. Comput. Methods Appl. Mech. Eng. **197**(49–50), 4104–4124 (2008)
20. Echter, R., Oesterle, B., Bischoff, M.: A hierarchic family of isogeometric shell finite elements. Comput. Methods Appl. Mech. Eng. **254**, 170–180 (2013)
21. Park, H., Kim, K.: Smooth surface approximation to serial cross-sections. Comput. Aided Des. **28**(12), 995–1005 (1996)